Trapping and cooling of $Sr^+$ ions: strings and large clouds



2009 J. Phys. B: At. Mol. Opt. Phys. 42 154014

(http://iopscience.iop.org/0953-4075/42/15/154014)

J. Phys. B: At. Mol. Opt. Phys. **42** (2009) 154014 (7pp) doi:10.1088/0953-4075/42/15/154014

# Trapping and cooling of $Sr^+$ ions: strings and large clouds

**S Removille, R Dubessy, B Dubost, Q Glorieux, T Coudreau, S Guibal, J-P Likforman and L Guidoni**

Laboratoire Matériaux et Phénoménes Quantiques, Université Paris Diderot et CNRS, UMR 7162, Bât. Condorcet, 75205 Paris Cedex 13, France

E-mail: luca.guidoni@univ-paris-diderot.fr

Received 17 February 2009, in final form 30 March 2009
Published 15 July 2009
Online at stacks.iop.org/JPhysB/42/154014

**Abstract**

This paper reports on trapping and laser cooling of singly ionized strontium ions in a linear Paul trap. We describe the loading technique based on two-photon absorption of femtosecond pulses at a wavelength of 431 nm and we compare this technique to electron-bombardment ionization. We perform Doppler cooling of the ions in the few-ions regime as well as in the case of large clouds. The analysis of the fluorescence spectra and direct imaging of the cloud allows us to identify the Coulomb-crystal regime. These experiments open the way to the use of a large cold trapped-ion cloud as a medium for quantum optics and quantum information experiments.

(Some figures in this article are in colour only in the electronic version)

## 1. Introduction

Samples of laser-cooled ions confined in electromagnetic traps play a prominent role in several domains related to atomic physics, such as quantum information [1], metrology [2] and quantum optics [3].

In the specific domain of quantum information, following the idea of Cirac and Zoller [4], small ion samples in a Coulomb-crystal state opened the way to many successful experiments on two-qubit entanglement and quantum gates [1]. Such experiments are performed in stiff linear Paul traps in which a radio-frequency (rf) electric field is used to confine the ions. The vibrational state of the ions is then manipulated by laser–ion interaction at the single-ion level.

In a quite different regime, large ion samples can be cooled down to the Coulomb-crystal phase in linear Paul traps [5, 6]. Such samples can be used as thermal baths for large molecules [6] and display very peculiar properties concerning their crystalline order [7] and related thermodynamical properties [8]. Some recent proposals deal with the use of this particular system as a medium for quantum optics [9] and quantum information experiments [10].

In this paper we present an experiment in which we create both small ion strings and large $Sr^+$ Coulomb ion-crystals. The setup is designed to obtain optically dense clouds in the perspective of an ion-based quantum memory for continuous variables [10]. The paper is organized as follows: in the first section we describe the technical aspects of the experimental setup (photoionization loading, trap geometry, laser cooling sources). We present in the second section the experimental results concerning the photoionization, the spectral characterization of the clouds and the characterization obtained by image analysis. We then conclude with some perspectives on absorption measurements in dense ion clouds.

## 2. Experimental setup

### 2.1. Photoionization of neutral Sr

As in many trapped-ion experiments, we use an alkaline earth element. These atoms, when deprived of an electron, have an electronic structure similar to the alkaline elements that are easily manipulated with laser beams (figure 1(c)). The abundance of the four natural isotopes of strontium ($^{84}$Sr, $^{86}$Sr, $^{87}$Sr, $^{88}$Sr) are respectively 0.56%, 9.86%, 7% and 82.58%. In what follows we will address the case of the most abundant isotope $^{88}$Sr, but the presence of other isotopes shows up in some experiments.

The traditional method used to load an ion trap with the desired species is to create the ions directly inside the

 

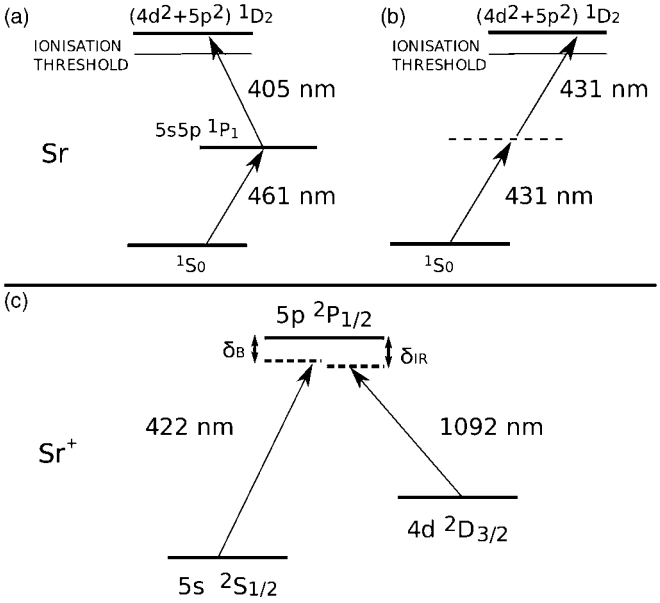


**Figure 1.** Relevant energy levels of neutral strontium involved in: (a) two-step photoionization, (b) two-photon photoionization (TPPI) discussed in this paper and (c) relevant energy levels of $Sr^+$ ion involved in Doppler cooling.

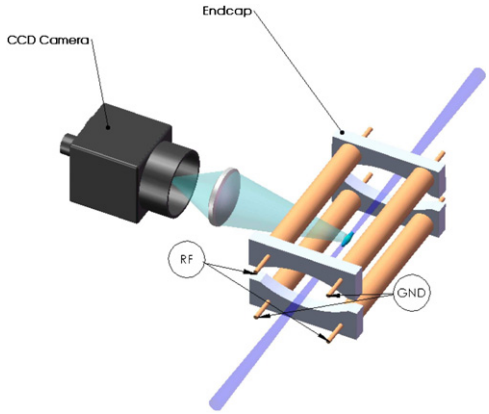


**Figure 2.** Schematic description of the linear Paul trap setup. Four parallel rods are used for the rf radial confinement ($r_0 = 3.2$ mm). Two 'end caps' separated by 30 mm are used for the longitudinal confinement. The trapped ions can be axially ejected and counted by an electron multiplier. The ion cloud fluorescence resulting from Doppler cooling is recorded by a CCD camera or by a photo-multiplier tube.

trapping region by electron-bombardment (EB) of a neutral atomic beam. As already underlined by several groups [11–13] this technique has serious drawbacks that can be eliminated by photoionization-based loading techniques. The relevant level structure of the neutral Sr atom is represented in figure 1(a). The $^1P_1$ intermediate level has been used to implement two-step photoionization [14, 13], following the example of Ca [11] and Yb [15]. In the particular case of the Sr atom, the presence of a $(4d^2 + 5p^2)^1D_2$ autoionizing state [16] provides a dramatic resonant enhancement of the photoionization efficiency. Such an autoionizing state can also be reached from the ground state by two-photon absorption [17–19]: the $(5s^2)^0S_0 \rightarrow (4d^2+5p^2)^1D_2$ two-photon transition has a linewidth of 0.7 nm FWHM (due to the short lifetime of the final state) and can be resonantly driven by two photons centred at 431 nm. Our loading strategy consists in using ultrafast pulses to drive such a two-photon transition (figure 1(b)). Our choice is motivated by the relative simplicity of the method that does not require laser stabilization and by the efficiency of ultrafast pulses for frequency doubling and two-photon absorption. Let us also mention that, because of its two-photon character, two-photon photoionization (TPPI) has the advantage of defining a well-localized spatial region for the ion production associated with the waist of the ionizing beam [21].

The neutral Sr atomic beam is produced in an oven formed by a tungsten filament in which flows a maximum current of 1.15 A, that corresponds to a heating power of 1.3 W. The temperature of the (bare) filament displays an approximate linear dependence on the current and we measured 110 °C for 0.8 A and 170 °C for 1.2 A. In these conditions we expect an Sr partial pressure roughly in the range $10^{-13}$–$10^{-9}$ mbar [22]. An electron gun based on a thorium tungsten wire allows us to perform EB with a typical electron energy of ≃300 eV. The photoionizing laser source is based on a homemade femtosecond Ti:Sa oscillator that produces ≃50 fs pulses of 1.5 nJ energy at 862 nm with a repetition rate of 100 MHz. The pulses are frequency doubled in a 0.5 mm thick beta barium borate (BBO) nonlinear crystal. The thickness of the crystal is such that group velocity mismatch negligibly affects pulse duration. A pulse energy of more than 0.15 nJ is routinely obtained at 431 nm. The beam is sent into the vacuum chamber and focused at the centre of the ion trap by a plano-convex lens of focal length 200 mm. The measured photoionizing beam size at the waist is $20 \pm 2$ $\mu$m, corresponding to a peak intensity of ≃1 GW cm$^{-2}$.

### 2.2. *Linear Paul trap*

$Sr^+$ ions are trapped in a standard linear Paul trap (see figure 2) [23]. Four parallel rod electrodes (diameter 6.35 mm, inner radius $r_0 = 3.2$ mm) are used for the radio-frequency (rf) radial confinement. A 2.1 MHz rf potential with an amplitude $V_{rf}$ in the range 50–500 V is applied to two of the diagonally opposed electrodes. The remaining two rods are normally grounded or used to resonantly excite the ion motion in the trap (see below). The $Sr^+$ ion radial movement is defined by a typical secular frequency $\nu_R = 300$ kHz for an applied voltage $V_{rf} = 500$ V. Two 'end caps' separated by 30 mm are used for the longitudinal confinement and brought to a static positive voltage $V_{ec}$ in the range 1–300 V. The corresponding axial frequency is $\nu_A$ is in the range 10–100 kHz. Trapped ions can be detected in a destructive way by an ejection sequence: an asymmetric potential is applied to the 'end caps' that kicks out the cloud along the trap axis through a set of electrodes which bend the ion trajectories and focus them on an electron multiplier. This detection scheme allows us to perform ion counting and to analyse the trapped species by performing mass spectra. A mass spectrum is obtained by measuring the losses induced in successive

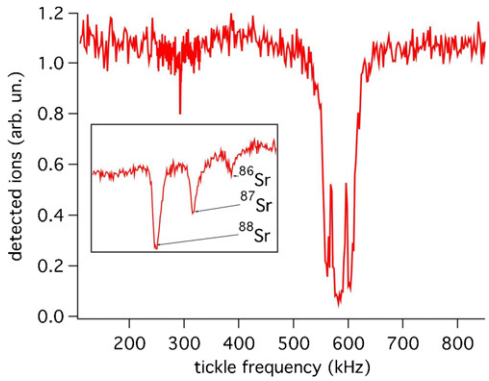


**Figure 3.** The mass spectrum of the trapped $Sr^+$ ion clouds produced by photoionisation. The two main peaks associated with $Sr^+$ are observed for a tickle frequency of $2\nu_R$ and $\nu_R$ (negative peaks in the mass spectrum). $V_{rf} = 500$ V. Inset: high resolution spectrum centred at $\nu_R = 290$ kHz. The three peaks corresponding to the three more abundant isotopes ($^{88}$Sr, $^{87}$Sr, $^{86}$Sr) are clearly distinguishable.

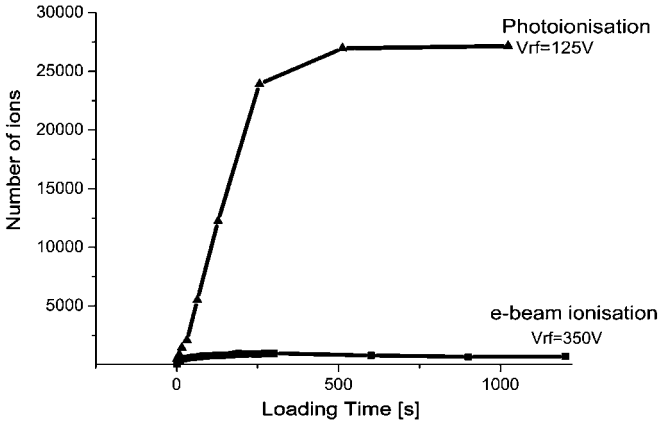


**Figure 4.** Number of trapped ions as a function of the loading time obtained by EB and TPPI. In the case of photoionization, the curve corresponds to $V_{rf} = 125$ V; in the case of electron bombardment $V_{rf} = 350$ V.

realizations of the cloud in the presence of a sinusoidal excitation ('tickle') applied to two diagonally opposed rods. The result of this parametric excitation is a depletion of the ion signal when the tickle frequency matches an integer fraction of $2\nu_R$ (negative peak in the mass spectrum) [24]. An example of such a mass spectrum obtained by photoionization loading of $Sr^+$ ions is reported in figure 3. In order to appreciate the mass selectivity of the method, we show in the inset a mass spectrum obtained with an increased resolution in which the contributions of the three most abundant $Sr^+$ isotopes are resolved.

### 2.3. Doppler laser cooling

Trapped $Sr^+$ ions are Doppler cooled using the $^2S_{1/2} \rightarrow {}^2P_{1/2}$ optical transition at 422 nm (natural linewidth, $\Gamma/2\pi = 20.2$ MHz, figure 1(c)). This transition is driven using laser light generated by a commercial extended-cavity diode laser (Toptica DL100) that delivers a maximum power of $\simeq$10 mW. In order to stabilize the laser frequency, we take advantage of the near-coincidence between the $^{88}Sr^+ {}^2S_{1/2} \rightarrow {}^2P_{1/2}$ and the $^{85}$Rb $5s\,{}^2S_{1/2}(F = 2) \rightarrow 6p\,{}^2P_{1/2}(F' = 3)$ transitions ($-440$ MHz) [25, 26]. We shift the laser frequency with a double-pass acousto-optic modulator and lock the laser frequency on a Doppler-free saturated-absorption signal obtained in a Rb cell.

A commercial 'repumping' fibre-laser (Koheras Adjustik Y10) at 1092 nm drives the $^2D_{3/2} \rightarrow {}^2P_{1/2}$ transition to avoid the accumulation of the ions (optical pumping) into the metastable $^2D_{3/2}$ state. This laser has a specified line width of 70 kHz and is used without external stabilization (estimated drift $<$100 MHz $h^{-1}$). A residual magnetic field on the order of $10^{-4}$ T defines a quantization-axis tilted with respect to the propagation axis of the linearly polarized repumping laser beam. This configuration prevents the ions from being optically pumped into a metastable dark state [26, 27].

## 3. Results

### 3.1. Trap loading

As mentioned above, the trap loading by a photoionization technique should eliminate several drawbacks (for instance the drift of the compensation voltages and the need to use high atomic fluxes). In order to test the performances of our loading scheme, we compared the loading times and the maximum number of trapped ions in the two cases of EB and TPPI.

The experiment is performed as follows: we turn-on the electron gun (or the photoionizing beam) and the cooling lasers at time $t = 0$; after a given time $\tau$, we turn off the electron gun (photoionizing beam) and we let the trapped cloud freely evolve for $\simeq$100 ms. We then turn off the cooling lasers (the strong damping due to the laser cooling reduces the ejection efficiency) and eject the ions towards the ion counter. We show in figure 4 the number of trapped ions, as a function of $\tau$, obtained using the two techniques. In both cases, saturation in the number of trapped ions is reached within a few tens of seconds. However, only TPPI allowed us to create a pure $Sr^+$ cloud containing a large number of ions: the EB technique saturates at around 1000 trapped ions. In fact, in this experiment, TPPI allowed the loading of $3 \times 10^4$ trapped $Sr^+$ ions, obtained for $V_{rf} = 125$ V. In the case of EB it is impossible to explore the same range for the parameter $V_{rf}$ without affecting the sample purity, since too many spurious ionic species, of mass lower than Sr, are produced and trapped at low RF voltages. Let us also remark that the selectivity against spurious molecules of the TPPI technique allowed us to load pure $Sr^+$ clouds in the trap at very low oven temperatures (on the order of 120° C), contrary to the case of EB (on the order of 165 °C).

### 3.2. Fluorescence spectra

As demonstrated in the very first experiments on ion Coulomb crystals [28], the measurement of the fluorescence of an ion cloud as a function of the detuning $\delta_B$ of the cooling laser gives precious information about the thermodynamic

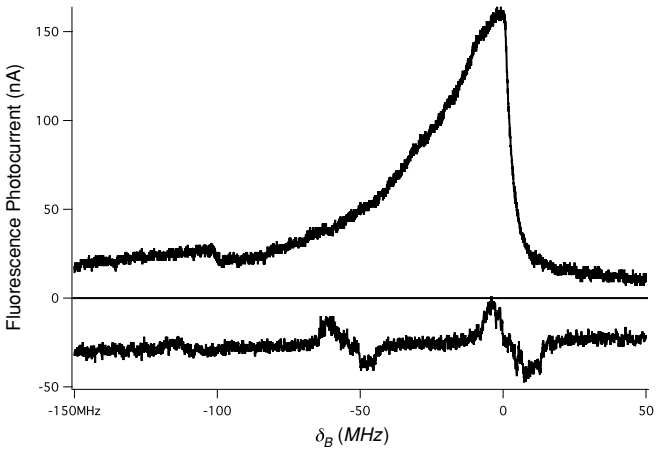


**Figure 5.** Fluorescence of a $Sr^+$ ion cloud as a function of the cooling laser detuning $\delta_B$ spanned at a constant rate of 20 MHz $s^{-1}$. The bottom trace (saturated absorption in a Rb cell) gives us the absolute frequency reference. The spectral feature (dip) around $-100$ MHz is attributed to a phase transition of the cloud. The repumping laser detuning is $\delta_{IR} > 0$.

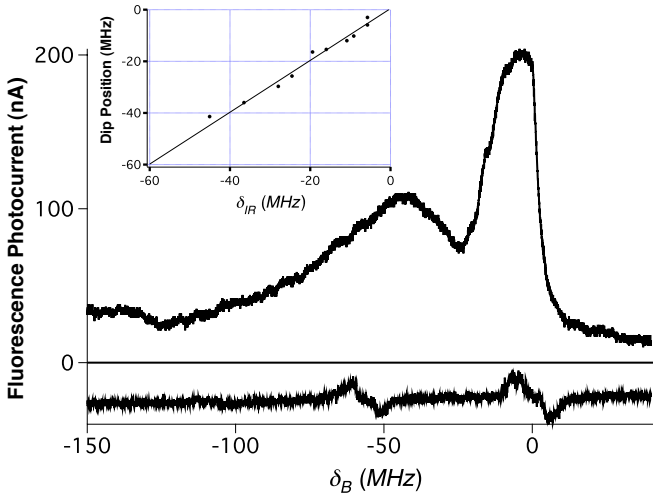


**Figure 6.** Fluorescence of a $Sr^+$ ion cloud as a function of the cooling laser detuning $\delta_B$. The repumping laser detuning is $\delta_{IR} = -25$ MHz. A two-photon dark resonance induces a dip in the spectrum. This resonance should occur when $\delta_B = \delta_{IR}$. The inset shows that the dip position follows exactly $\delta_{IR}$.

phase of the cloud and an estimate of its temperature. The integrated fluorescence of the ion cloud is detected using a photomultiplier. Fluorescence spectra are realized by scanning the cooling laser and recording simultaneously the fluorescence level and the saturated absorption of $^{85}$Rb that provides an absolute frequency reference. In figure 5 we show a typical fluorescence spectrum of a large $Sr^+$ cloud ($\simeq$1000 ions) as a function of the detuning $\delta_B$. This kind of spectrum exhibits non-trivial shapes because the laser detuning has an influence both on the cooling efficiency (and thus on the Doppler broadening) and on the excitation rate. These two effects are coupled and one can observe a sharp variation of the fluorescence at the atomic resonance. The overall asymmetric form (roughly half-Lorentzian) of the spectrum with an edge corresponding to $\delta_B = 0$ is due to the Doppler heating mechanism present for $\delta_B > 0$. The half-width of the spectrum is close to the natural linewidth, as expected in the case of crystalline Doppler-cooled clouds (Doppler broadening negligible with respect to natural linewidth). The spectral feature (dip) around $-100$ MHz is attributed to a phase transition of the cloud that occurs when the cooling power exceeds the rf heating resulting in a fast cooling of the sample [29] that changes the Doppler width of the spectrum. Let us recall that such a diagnostic is often used [30] but that the exact interpretation of the dip (Coulomb crystal versus liquid phase) can only be done by a simultaneous image analysis [31]. This phase transition observed in the spectrum is also present in the ion-cloud shape as described below. The shape and the width of this kind of spectrum critically depend on the spanning rate of the cooling laser, due to the characteristic cooling time that becomes very long (on the order of several seconds) for very large clouds. Therefore, scanning has to be slow compared to thermalization time; in our experiments this condition is fulfilled for scanning rates slower than 60 MHz $s^{-1}$. Indeed for very low cooling power and large $V_{RF}$ the spectra display perfectly symmetric Gaussian shapes with a width of several GHz, corresponding to a cloud temperature of $\simeq$6000 K. As expected, this temperature value is on the order of the potential depth of the trap.

Depending on the detuning $\delta_{IR}$ of the repumping laser, a dip can also be observed on the low-frequency edge of the resonance which is attributed to a dark state, coherent superposition of S and D Zeeman sub-levels coupled by the cooling and the repumping lasers (figure 6) [20, 27]. When the two-photon resonance condition is realized, a fraction of the ion population is coherently trapped in dark states. Such ions are no longer coupled to the excited P state and the fluorescence rate decreases. Figure 7 shows the variation of the position of this dark-state dip in the fluorescence spectrum as a function of the repumping laser frequency, confirming the two-photon resonance condition.

### *3.3. Imaging techniques*

A key diagnostic tool in an experiment dealing with trapped ions is the fluorescence image of the clouds. For example, the detection of the spatially resolved ion fluorescence in small ion strings is the basis of reliable and efficient qubit state measurements [32]. The analysis of the shape in the case of a macroscopic ion cloud allowed us to estimate several characteristics of the cloud: the ion motional frequencies, the number of trapped ions, the ensemble state (thermal cloud or crystallized ensemble).

*3.3.1. Ion strings.* The number of trapped ions can be controlled very accurately (one-by-one) by varying the loading time (typically 1 s) and the strontium oven temperature. Depending on the trap parameters (radial and axial secular frequencies) and the number of ions, one can observe ion strings (figures 7 and 8) or small crystallized clouds. The typical inter-ion distance is the range of tens of microns. In some experiments, dark holes in the string are observed between two fluorescent ions separated by twice the average

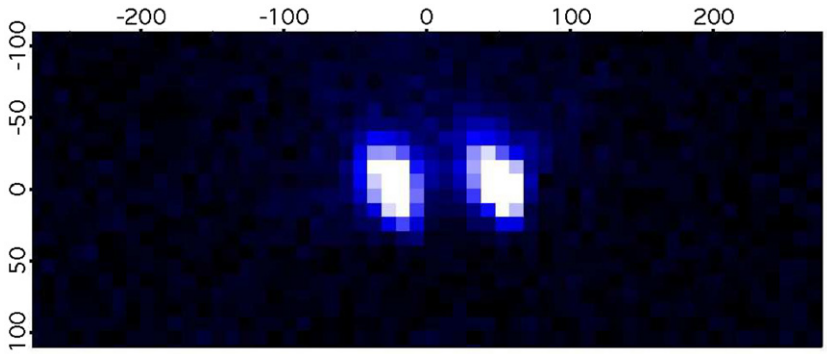


**Figure 7.** Two ions crystallized along the trap axis, exposure time: 2 s, magnification ×0.65 (axis scales in microns). The maximum photon count is found for $\delta_B \simeq -\Gamma$ and $\delta_{IR} \simeq 0$. The distance between the two ions is 80 $\mu$m. A commercial Canon zoom lens 70–200 mm $f/2.8$ has been used to form the image of the ions on a Roper Coolsnap EZ CCD camera.

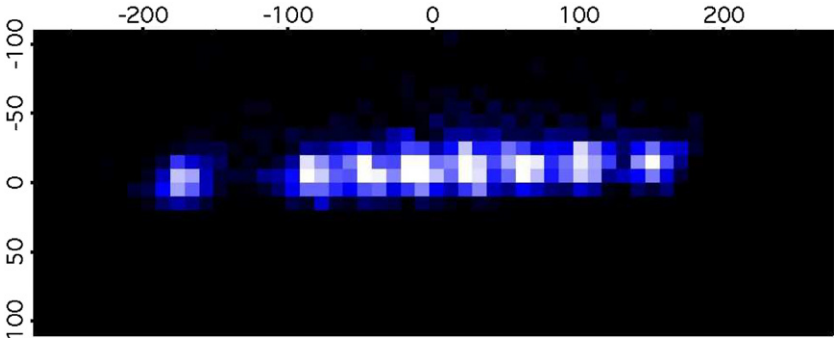


**Figure 8.** Eight bright ions and one dark ion (hole in the string structure) forming a small linear Coulomb cluster. The average distance between the ions is 36 $\mu$m.

inter-ion distance (figure 8). These 'defects' are attributed to the presence in the trap of ions which are not optically excited by the cooling laser. These dark ions are most likely other strontium isotopes trapped during the loading phase, but may also originate from chemical reactions of trapped $^{88}$Sr ions with residual molecules present in the vacuum system, leading to the formation of presumably $SrH^+$ molecular ions. These trapped molecules are not directly laser cooled but can be sympathetically cooled by their electrostatic interaction with $^{88}$Sr ions. Similar chemical reactions have been reported in the case of Mg or Ca trapped ions [33]. The study of a small ion cloud containing $\simeq$100 ions showed a relative fluorescence rate decrease of approximately 30% in 2 h whereas the total number of ions detected by ion counting did not vary notably. We interpret this behaviour in terms of a photo-assisted chemical reaction that replaces the initially trapped $^{88}Sr^+$ by molecular ions. The photo-assisted character of this chemical reaction is suggested by the results of the same experiment carried out without cooling that did not exhibit such a fluorescence rate variation after the same delay.

The analysis of the fluorescence image (figure 7), allows us to measure the fluorescence rate of an ion in a small chain. The calculation is performed taking into account the imaging system collection angle (0.09 sr), the CCD camera sensitivity (14 photons per CCD count per second per pixel), the exposure time (2 s), the losses of our imaging system (50%). We find that an individual ion emits a maximum of $4.7 \times 10^6$ photons per second to be compared to the natural linewidth of 20.2 MHz. We conclude that, when maximizing the fluorescence of the two-ion chain, the excited-state population is as high as 23%.

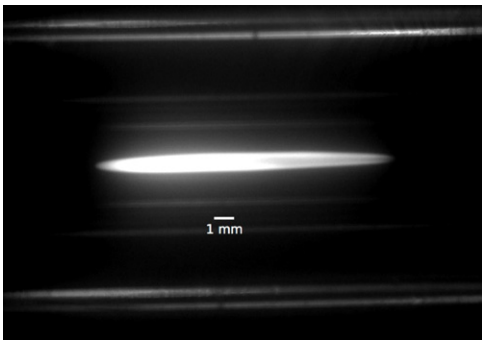


**Figure 9.** Fluorescence image of a 14 mm long $Sr^+$ Coulomb crystal containing $\simeq$90 000 ions. Experimental parameters: $V_{rf} = 130$ V, $V_{ec} = 4$ V.

*3.3.2. Large ion clouds.* Large ion clouds are obtained by increasing the loading time to several minutes in the presence of the cooling lasers. Figure 9 displays a typical image of such a cloud. The cloud shape depends on its temperature, displaying a phase transition from a disordered sample governed by a thermal distribution to a crystallized one. Following the analysis of [28], we introduce the ratio $\Gamma = \frac{e^2}{4\pi\epsilon_0 a k_B T}$ between mean Coulomb repulsion energy and mean kinetic energy (here $a$ is the mean distance between two

neighbouring ions, defined by $\frac{4\pi}{3}a^3 n_0 = 1$, with $n_0$ the ion density). One may separate two different regimes.

For $\Gamma \ll 1$, the high average kinetic energy limit, the cloud profile is governed by a thermal distribution in a harmonic potential displaying Gaussian wings. For $\Gamma \gg 1$, the strong Coulomb coupling regime, the fluorescence profile displays a flat-top sharp-edge profile. In this latter case, we may estimate an upper bound for the ion density [8] given by:

$$n_0 = \frac{m\epsilon_0}{e^2}\left(2\omega_r^2 + \omega_z^2\right), \quad (1)$$

where $\omega_r$, $\omega_z$ are the secular frequencies of the ions movement along the radial and axial directions. Then the total number of ions is: $N = n_0 V$, where $V$ is the volume of the cloud, extracted from the image.

The experimental determination of $\omega_r$ and $\omega_z$ is made through resonant excitation of the ion motion by applying small-amplitude (typically a few mV) variable-frequency sinusoidal voltage to the trapping electrodes. While scanning the frequency of this excitation, one resonantly excites the vibrations of the cloud, heating up the ions. This results in a change of the shape of the cloud, with sharp resonances when the excitation frequency is close to the trap secular frequencies.

In the case of the crystallized cloud shown in figure 9, we measure a radius of $r_0 = 400$ $\mu$m, a half-length of $z_0 = 6.8$ mm, $\frac{\omega_r}{2\pi} = 70$ kHz and $\frac{\omega_z}{2\pi} = 11$ kHz. Therefore the maximal number of ions in the cloud is: $N_{\max} \simeq 9 \times 10^4$. This ion number determination, although less accurate than the ion-counting method presented above, has the advantage of being *in situ* and non-destructive.

## 4. Conclusion

We presented an experimental setup devoted to trapping and laser cooling of large clouds of singly ionized strontium ions in a linear Paul trap. In particular we described a loading technique based on two-photon absorption of femtosecond pulses at a wavelength of 431 nm that we compared to electron-bombardment ionization. This technique allowed us to obtain clouds containing $\simeq 9 \times 10^4$ ions. We analysed Doppler-cooled samples of ion Coulomb crystals both in the few-ion regime and in the case of large clouds using several diagnostic tools based on direct ion detection (electron multiplier), integrated fluorescence spectra and CCD image analysis.

Taking into account experimental ion density and the absorption cross-section ($2.8 \times 10^{-14}$ m$^2$), we found an optical depth at resonance $\alpha l = 0.5 \times 10^{-2}$. Preliminary measurements of the absorption spectra of an axial resonant probe are in good agreement with this estimation. As already analysed in [10], the required $\alpha l$ for realizing a medium suitable for a single-pass quantum memory is in the range of 10. Trapping an increased number of ions (a factor 20 more) in a smaller volume (radius divided by 10) will be achieved by increasing the stiffness of the trap potentials while maintaining a favourable balance between the rf-heating-rate and the laser-cooling power in order to keep the ion cloud crystallized. These improvements on the experimental setup will pave the way for using a large cold trapped-ion cloud as a medium for quantum optics and quantum information experiments, in particular the realization of a long-lived quantum memory.

## Acknowledgments

We thank P Lepert for technical support. Many thanks to David Lucas for enlightening discussions and for his precious help with the experiments on hot clouds. The authors would also like to thank M Joffre for lending the femtosecond oscillator used for photoionization experiments. This work was supported by ANR 'jeunes chercheuses et jeunes chercheurs' research contract JC05_61454.

## References

[1] Häffner H, Roos C F and Blatt R 2008 Quantum computing with trapped ions *Phys. Rep.* **469** 155
Blatt R and Wineland D 2008 Entangled states of trapped atomic ions *Nature* **453** 1008
Coudreau T 2009 Recent experiments in quantum information with trapped ions *J. Phys. B: At. Mol. Opt. Phys.* **42** 154011

[2] Gill P 2005 Optical frequency standards *Metrologia* **42** S125–37

[3] Guthöhrlein G R, Keller M, Hayasaka K, Lange W and Walther H 2001 A single ion as a nanoscopic probe of an optical field *Nature* **414** 49
Eschner J, Raab C, Schmidt-Kaler F and Blatt R 2001 Light interference from single atoms and their mirror images *Nature* **413** 495
Herskind P, Dantan A, Langkilde-Lauesen M B, Mortensen A, Sørensen J L and Drewsen M 2008 Loading of large ion Coulomb crystals into a linear Paul trap incorporating an optical cavity *Appl. Phys.* B **93** 373–9

[4] Cirac I and Zoller P 1995 Quantum computations with cold trapped ions *Phys. Rev. Lett.* **74** 4091

[5] Drewsen M *et al* 1998 Large ion crystals in a linear Paul trap *Phys. Rev. Lett.* **81** 2878

[6] Ostendorf A, Zhang C B, Wilson M A, Offenberg D, Roth B and Schiller S 2006 Sympathetic cooling of complex molecular ions to millikelvin temperatures *Phys. Rev. Lett.* **97** 243005
Ostendorf A, Zhang C B, Wilson M A, Offenberg D, Roth B and Schiller S 2008 Sympathetic cooling of complex molecular ions to millikelvin temperatures *Phys. Rev. Lett.* **100** 019904 (erratum)

[7] Mortensen A, Nielsen E, Matthey T and Drewsen M 2006 Observation of three-dimensional long-range order in small ion Coulomb crystals in an rf trap *Phys. Rev. Lett.* **96** 103001

[8] Dubin D H and O'Neil T M 1999 *Rev. Mod. Phys.* **71** 87

[9] Herskind P, Dantan A, Langkilde-Lauesen M B, Mortensen A, Sørensen J L and Drewsen M 2008 Loading of large ion Coulomb crystals into a linear Paul trap incorporating an optical cavity *Appl. Phys.* B **93** 373

[10] Coudreau T, Grosshans F, Guibal S and Guidoni L 2007 Feasibility of a quantum memory for continuous variables based on trapped ions: from generic criteria to practical implementation *J. Phys. B: At. Mol. Opt. Phys.* **40** 413 http://dx.doi.org/10.1088/0953-4075/40/2/014

[11] Gulde S, Rotter D, Barton P, Schmidt-Kaler F, Blatt R and Hogervorst W 2001 Simple and efficient photo-ionisation loading of ions for precision ion-trapping experiments *Appl. Phys.* B **73** 861–3 http://dx.doi.org/10.1007/s003400100749

[12] Lucas D M, Ramos A, Home J P, McDonnell M J, Nakayama S, Stacey J-P, Webster S C, Stacey D N and Steane A M 2004 Isotope-selective photoionisation for

calcium ion trapping *Phys. Rev.* A **69** 012711 http://dx.doi.org/10.1103/PhysRevA.69.012711

[13] Brownnutt M, Letchumanan V, Wilpers G, Thompson R C, Gill P and Sinclair A G 2007 Controlled photoionisation loading of $^{88}Sr^{+}$ for precision ion-trap experiments *Appl. Phys.* B **87** 411–5 http://dx.doi.org/10.1007/s00340-007-2624-8

[14] Vant K, Chiaverini J, Lybarger W and Berkeland D J 2006 Photoionization of strontium for trapped-ion quantum information processing arXiv:quant-ph/0607055v1

[15] Hosaka K, Webster S A, Blythe P J, Stannard A, Beaton D, Margolis H S, Lea S N and Gill P 2005 An optical frequency standard based on the electric octupole transition in $^{171}Yb^{+}$ *IEEE Trans. Instrum. Meas.* **54** 759–62

Balzer Chr, Braun A, Hannemann T, Paape Chr, Ettler M, Neuhauser W and Wunderlich Chr 2006 Electrodynamically trapped $Yb^{+}$ ions for quantum information processing *Phys. Rev.* A **73** 041407

[16] Mende W, Bartschat K and Kock M 1995 Near-threshold photoionization from the Sr I (5s5p) $^{1}P_{1}^{0}$ state *J. Phys. B: At. Mol. Opt. Phys.* **28** 2385–93

[17] Baig M A, Yaseen M, Ali R, Nadeem A and Bhatti S A 1998 Near-threshold photoionisation spectra of strontium *Chem. Phys. Lett.* **296** 403–8

[18] Kirlov E and Putterman S 2007 2-photon ionization and necessary laser and vacuum systems for experiments with trapped strontium ions arXiv:0712.0222v1

[19] Removille S, Dubessy R, Glorieux Q, Guibal S, Coudreau T, Guidoni L and Likforman J-P 2008 Photoionisation loading of large $Sr^{+}$ ion clouds with ultrafast pulses arXiv:0811.3399

[20] Siemers I, Schubert M, Blatt R, Neuhauser W and Toschek P E 1992 The 'trapped state' of a trapped ion–line shifts and shape *Europhys. Lett.* **18** 139–44

[21] Diaspro A (ed) 2001 *Confocal and Two-Photon Microscopy: Foundations, Applications and Advances* (Weinheim: Wiley) ISBN 0-471-40920-0

[22] Nesmeyanov A N 1963 *Vapour Pressure of the Elements* (London: Infosearch) pp 185–7

[23] Prestage J D, Dick G J and Maleki L 1989 New ion trap for frequency standard applications *J. Appl. Phys.* **66** 1013 http://dx.doi.org/10.1063/1.343486

[24] Guidoni L, Guibal S, Coudreau T, Dubost B and Grosshans F 2006 Dynamique d'ions confinés dans un piége de Paul linéaire *J. Phys. IV France* **135** 315–6 http://dx.doi.org/10.1051/jp4:2006135104

[25] Madej A A, Marmet L and Bernard J E 2004 Rb atomic absorption line reference for single $Sr^{+}$ laser cooling systems *Appl. Phys.* B **67** 229

[26] Sinclair A G, Wilson M A and Gill P 2001 Improved three-dimensional control of a single strontium ion in an endcap trap *Opt. Comm.* **190** 193

[27] Berkeland D J and Boshier M 2002 Destabilization of dark states and optical spectroscopy in Zeeman-degenerate atomic systems *Phys. Rev.* A **65** 033413

[28] Diedrich G, Peik E, Chen Jun, Quint W and Walther H 1987 Observation of a phase transition of stored laser-cooled ions *Phys. Rev. Lett.* **59** 2931

[29] Blümel R, Kappler C, Quint W and Walther H 1989 Chaos and order of laser-cooled ions in a Paul trap *Phys. Rev.* A **40** 808

[30] Zhao X, Ryjkov V L and Schuessler H A 2006 Fluorescence profiles and cooling dynamics of laser-cooled $Mg^{+}$ ions in a linear rf ion trap *Phys. Rev.* A **73** 33412

[31] Hornekær L and Drewsen M 2002 Formation process of large ion Coulomb crystals in linear Paul traps *Phys. Rev.* A **66** 13412

[32] Myerson A H, Szwer D J, Webster S C, Allcock D T C, Curtis M J, Imreh G, Sherman J A, Stacey D N, Steane A M and Lucas D M 2008 High-fidelity readout of trapped-ion qubits *Phys. Rev. Lett.* **100** 200502

[33] Mølhave K and Drewsen M 2000 Formation of translationally cold $MgH^{+}/MgD^{+}$ molecules in an ion trap *Phys. Rev.* A **62** 0011401